BNL--34940

DE84 014698

STUDIES OF NEUTRON-RICH NUCLEI FAR FROM STABILITY AT TRISTAN

R. L. Gill
Brookhaven National Laboratory, Upton, New York 11973

ABSTRACT

The ISOL facility, TRISTAN, is a user facility located at Brookhaven National Laboratory's High Flux Beam Reactor. Short-lived, neutron-rich nuclei, far from stability, are produced by thermal neutron fission of ^{235}U. An extensive array of experimental end stations are available for nuclear structure studies. These studies are augmented by a variety of long-lived ion sources suitable for use at a reactor facility. Some recent results at TRISTAN are presented as examples of using an ISOL facility to study series of nuclei, whereby an effective means of conducting nuclear structure investigations is available.

THE TRISTAN FACILITY

A schematic layout of the TRISTAN ISOL facility is shown in Fig. 1. A neutron beam of about 3 x 10^{10} $n_{th}/cm^2/sec$ is provided by the 60 MW High Flux Beam Reactor at Brookhaven National Laboratory. Ion source development, as well as separator improvements, operation and maintenance is the responsibility of the Brookhaven TRISTAN staff. Experiments are performed by the Brookhaven staff, and an international group of users. Construction of experimental facilities has been done in collaborations of users and in-house staff. Ion sources of the surface ionization[1], negative surface ionization, thermal[2], FEBIAD[3], and high-temperature plasma ionization types are available to be placed in the neutron beam. Each source has an internal target. The FEBIAD ion source can contain 2.5g ^{235}U, whereas the other types can contain up to 10g ^{235}U. A 90° sector magnet provides the primary mass separation and a ±45° switch magnet gives some additional mass separation for the extreme angles as well as provides beam lines for 5 separate experimental stations.

A general purpose gamma-ray spectroscopy facility with a high-speed moving tape collector is available at one of the 45° lines. A 4-detector angular correlation system[4] may be positioned either at the point of ion beam deposit for short-lived activities, or at a downstream position for longer-lived activities. Q_β measurements can be made at this station using thin window HPGe (hyperpure Germanium) detectors.

A large, high-efficiency, polyethylene moderated ^{3}He counter is used for P_n, P_{2n} and $P_{2n}(\theta)$ measurements. A high resolution time-of-flight neutron spectrometer is also available to measure low energy neutron spectra.

Conversion electron spectra can be studied by using a windowless Si(Li) detector installed at the 0° position. A moving tape collector positions the deposited activity in front of the detector where electron singles, electron γ-ray coincidence and β-gated electron spectra can be simultaneously accumulated.

A colinear-fast beam dye laser facility is available to measure isotope shifts and other hyperfine interactions from nuclides in the ionic state. A quadrupole ion trap is under development for later use with the dye laser system.

ps

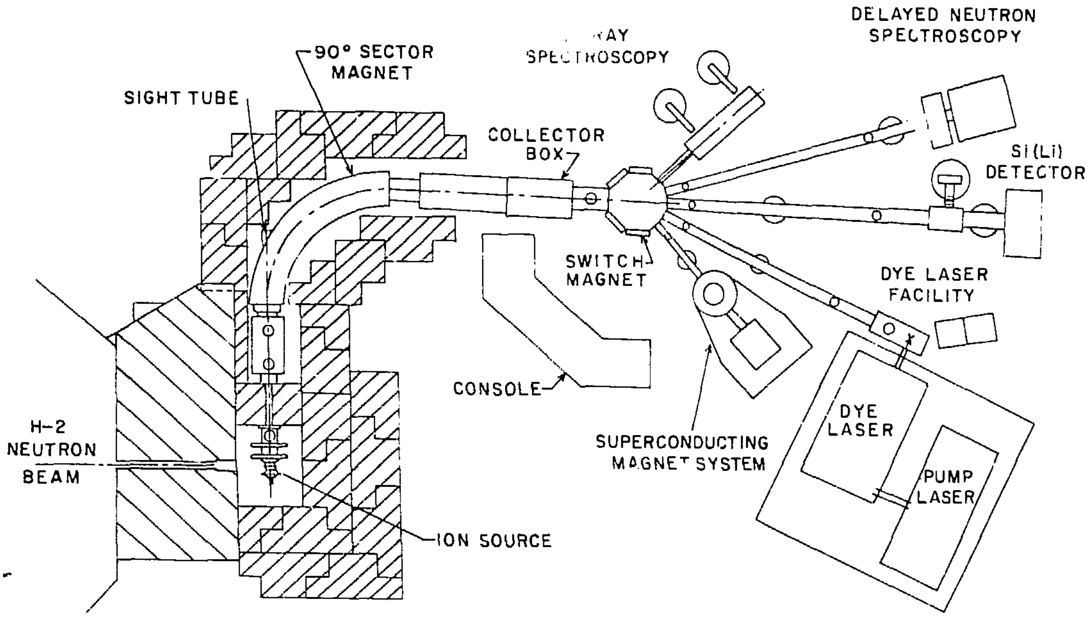

Fig. 1 Schematic layout of the current TRISTAN facility.

A split-pole superconducting magnet with a 6.25 Tesla field strength at 4.2°K is available for g-factor measurements. The magnet is equipped with a λ-point refrigeration unit which allows operation at 2.2°K, resulting in fields of up to 6.75 Tesla. The magnet was specially designed to be used as a solenoid magnet as an alternative configuration. By removing the lower pole piece and installing a HPGe detector, the solenoid field can be used to focus electrons from β decay onto the face of the detector, resulting in a large effective solid angle for betas, while maintaining a relatively small solid angle for gammas. This system is used for high sensitivity Q_β measurements.

An ion implantation facility is currently under development. This facility will include a post accelerator capable of boosting the total ion energy to about 200 keV. The goal of this project is to measure quadrupole moments of excited states by implanting radioactive ions in crystals with known electric field gradients. Implantation into ferromagnetic materials at low temperatures may also be attempted at later stages of the project.

ION SOURCES AT TRISTAN

Introduction

The primary emphasis on ion source development at TRISTAN has been to produce very long-lived, stable ion sources. The importance of long ion source lifetimes and stable operation is evident by considering that TRISTAN receives 24 days of neutron beam per month. Demands for beam time require that the separator operate continuously during that time period. Such a schedule (24 days on, 6 days off) is exhausting to both equipment and personnel, but makes it possible to perform long-term experiments that could not be attempted under other circumstances. Last year (1983), TRISTAN operated for greater than 90% of the available reactor time. To maintain this sort of performance, an ion source must reliably operate for one full cycle, preferably two. Thus, our goal for an ion source lifetime is 1200 hours, although 600 is acceptable.

All of the sources use highly enriched uranium targets, prepared by impregnating graphite or graphite cloth with uranyl nitrate, which is converted to uranium dioxide or uranium carbide at high temperatures. As noted above, the targets can continue up to 10g ^{235}U, resulting in very high levels of radioactivity, making frequent ion source changes undesirable.

Surface Ionization Source

The first successful ion source at TRISTAN was the surface ionization source developed by Shmid et al.[1] The source can be heated to >2000°C using 2500 W of electron bombardment power. Ionizing surfaces of Re and Ta have been used. Ta gives lower yields of Sr and Ba, making it more desirable than a Re ionizer for experiments on Rb and Cs decay. This source is fully developed and has lifetimes of >2500 hours. The surface ionization source allows experiments on beams of Rb, Sr, Y, Cs, Ba, Ce, and Pr and their decay products.

The FEBIAD Source

A FEBIAD source, modeled after that of Kirchner[5] is also in use. The source is modified to provide longer lifetimes and a larger target area to make use of the full size of the neutron beam. Lifetimes of up to 1500 hours have been achieved. The lifetime and wide array of elements available from this source have made it the source most used at TRISTAN. The ion source is shown in Fig. 2. The FEBIAD ion source allows experiments on beams of Cu, Zn, Ga, Ge, Se, Br, Kr, Rb, Ag, Cd, In, Sn, Sb, Te, I, Xe, and Cs and their decay products.

Thermal Ion Source

The TRISTAN thermal ion source is described in detail by Piotrowski et al.[2] This source was based on the TRISTAN surface ionization source and was the first of a "family" of ion sources which share a common design for the target, heater, base plate, and heat shields. This family of TRISTAN ion sources includes the thermal, negative and high-temperature plasma sources (to be described below). The targets use graphite or graphite cloth to contain the uranium in a tube which is heated by electron bombardment by a filament. The filament is supported by Ta wires which protrude through the heat shields and attach to insulators on the support rods. This construction is indicated in Fig. 3 which shows the thermal ion source. With this arrangement, the target can be heated to 2500°C with 1800 W of electron bombardment power. The thermal ion source allows experiments on beams of Ga, Ge, As, Rb, Sr, Y, In, Sn, Cs, Ba, La, Ce, Pr, Nd, Pm, Sm, Eu, Gd, Tb, Dy, and Ho and their decay products.

Negative Ion Source

The TRISTAN negative ion source produces beams of halogens (Br and I from neutron fission of ^{235}U). An important feature of this type of

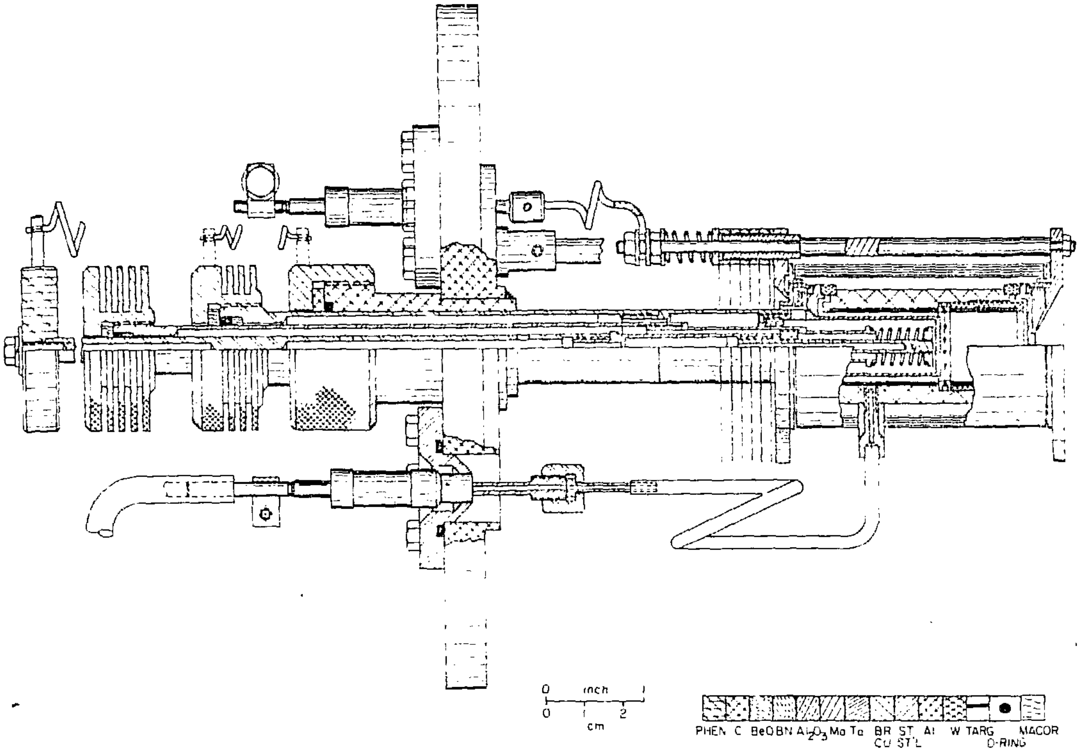

Fig. 2 The TRISTAN FEBIAD ion source.

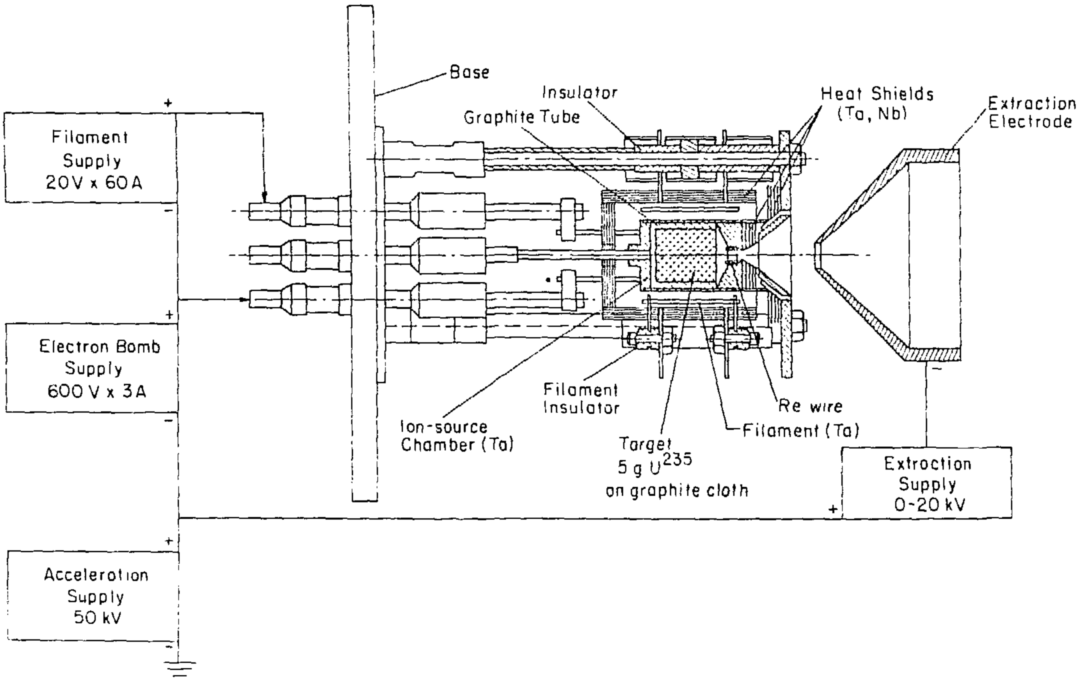

Fig. 3 The TRISTAN thermal ion source, showing the construction common to the family of sources.

source is that it produces only Br^- and I^-, so that experiments on low yield masses of Br and I can be studied without the intense interferences from Kr, Rb, Xe, and Cs. The source is constructed in the same fashion as the thermal ion source, except that the Ta/Re ionizer is replaced by a Ta tube with a LaB_6 ionizer. Electrons from the source are deflected by a permanent magnet and a plate with a 1000 V potential.

High Temperature Plasma Ion Source

Figure 4 shows the high temperature plasma ion source, where the heat shields are not shown to make the diagram more simple. This source represents a novel concept in ISOL ion sources in that the target is located (and is actually part of) the cathode. At operating temperatures (near 2500°C) electrons are emitted from the Ta chamber walls, from the target material and from an emitter disk over the target. The emitter disk also keeps graphite cloth in the target chamber from touching, and thereby short circuiting, the anode. The anode consists of W-wire grid which protrudes into the target/cathode chamber.

The high temperature at which this source operates gives much faster diffusion than the lower temperature FEBIAD source, and overall gives higher yields by a factor of 10. The anode in the high temperature plasma source has operated for a total of about 2000 hours without failure. All failures have been associated with the filament and heat shield configuration. The high temperature plasma ion source allows experiments on beams of Cu, Zn, Ga, Ge, As, Se, Br, Kr, Rb, Sr, Y, Ag, Cd, In, Sn, Sb, Te, I, Xe, Cs, Ba, Ce, and Pr and their decay products.

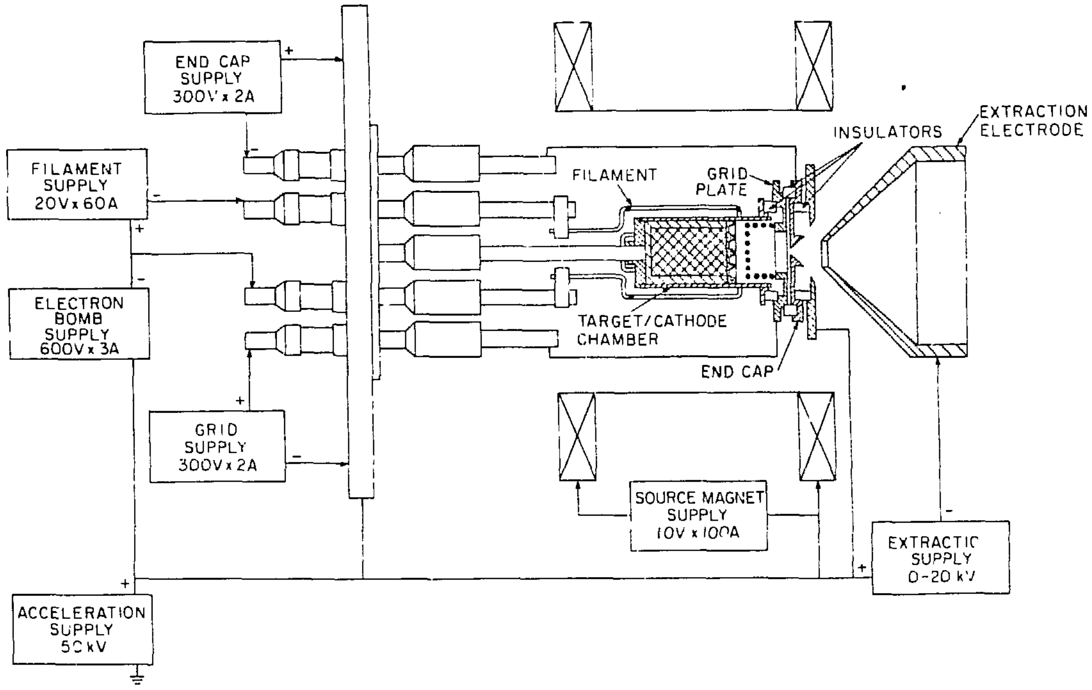

Fig. 4 The TRISTAN high temperature plasma ion source.

NUCLEAR STRUCTURE STUDIES AT TRISTAN

The ability to give access to extended sequences of nuclei is an inherent feature of any ISOL facility. Indeed, if a reaction produces only one product, there is usually no need for mass separation. This feature, by itself, gives ISOL facilities the unique ability to easily study the evolution of nuclear structure resulting from changes in the relative numbers of neutrons or protons in a many body system. In addition, by employing appropriate variations of targets, ion sources, and incident beams, nuclei which exhibit widely differing modes of excitation can be examined in detail. At some ISOL facilities, such as TRISTAN, both of these features can be provided by a single mechanism, usually fission. Fission provides access to nuclei both near stability and near the neutron (or proton) drip li [illegible] s access to nuclei near and at closed shells and in region [illegible]. The production of nuclei far from stability also make [illegible] exotic decay modes, such as delayed neutron and [illegible] 2- [illegible] ion. Some recent results at TRISTAN will be [illegible] in th [illegible] of this paper.

Parabolic Multiplets in N=83 Nuclides

Studies at TRISTAN have shown that the odd-odd N=83 nuclides can be interpreted almost entirely on the basis of a quadrupole interaction.[6] The analysis follows that of Paar[7] where p-n multiplets near single closed shells are described in terms of dipole and quadrupole interactions from which a parabolic relationship between E(I) and I(I+1) arises. The dominant factor in the energy arises from the quadrupole interaction and is determined by a quadrupole interaction strength parameter and an occupation number (V) that is +1 if the proton and neutron are both holes or both particles and −1 if one is a particle and the other a hole. The resulting parabola will open down if $V = +1$ and up if $V = -1$. The effect of the dipole interaction is linear in I(I+1) and has the effect of shifting the vertex of the parabola.

The results of fitting these multiplets is shown in Fig. 5. A total of 50 levels have been fit in four nuclides with an rms error of 17 keV. The agreement is best in the lowest lying multiplet and suggests that there is little configuration mixing in that multiplet. The dipole interaction strength was small and usually less than 10% of the quadrupole strength. The calculations have been extended to the N=85 nucleus ^{142}La with comparable success.

Deformed Odd-A Nuclei in the A≈100 Region

Six rotational bands with small and similar values of $h^2/2I$ have been found in ^{99,101}Y, ^{99}Sr and ^{101}Sr at TRISTAN.[8] Prior to this work, only one rotational band for an odd-A nucleus in this region has been reported. The rotational bands are shown in Fig. 6. Experimental values for $|(g_K-g_R)/Q_0|$ were obtained from branching ratios for intraband γ transitions under the assumption of pure K bands. These ratios can then be used to deduce a Nilsson orbital assignment for the band. For Y isotopes the only K = 5/2 orbitals near the Fermi surface for $\beta \approx 0.3$-0.4 are 5/2[422] and 5/2[303]. For neutrons, the only K = 3/2 orbitals expected near the Fermi surface for $\beta \approx 0.3$-0.4 are 3/2[411] and 3/2[541]. The K = 5/2 ground bands in the Y isotopes are well described by the 5/2[422] Nilsson state and the 570-keV band in ^{101}Y is most likely

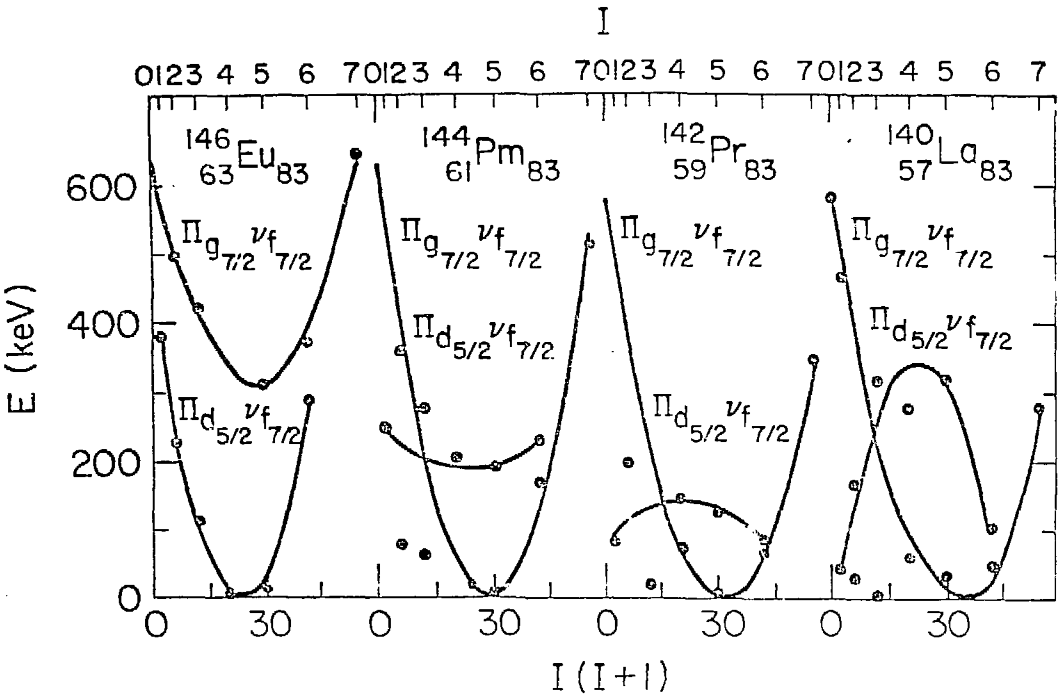

Fig. 5. The low-lying levels of the odd-odd N=83 nuclides. The experimental data are shown by solid points and the solid curves are the fitted paraboli.

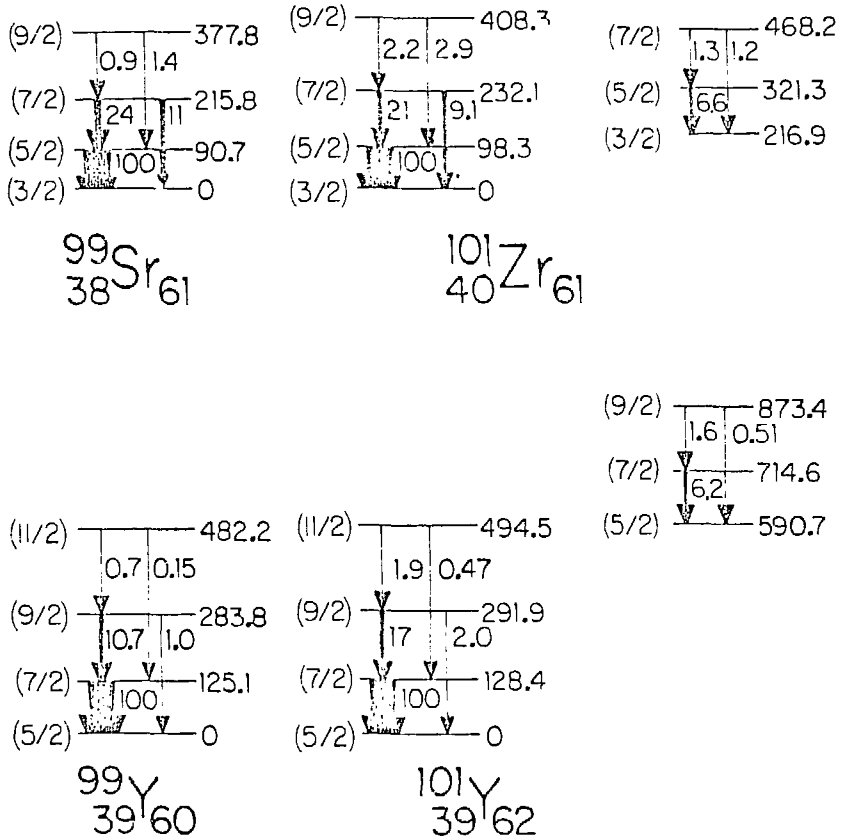

Fig. 6. Rotational bands in deformed odd-A Y isotopes and N=61 isotones. Intraband γ transitions and their relative intensities from β decay are shown.

$5/2[303]$. The probably existence of the $\pi 5/2[422]$ and $\nu 3/2[411]$ orbitals near the Fermi surface for highly deformed $A \approx 100$ nuclei is consistent with the concept that deformation is strongly promoted by occupation of neutron and proton orbitals with strong spatial overlap.

g-factor Measurements

An ongoing program to measure g-factors of excited states in nuclei far from stability at TRISTAN initially examined Ba isotopes near the Z=64 subshell closure.[9] In this study, the results obtained at TRISTAN were combined with results from others to investigate proton valence space truncation near the subshell gap. The simple formalism of the IBA-2 was used to predict g factors in this region. The M1 operator can be written

$$T(M1) = g_\pi L_\pi + g_\nu L_\nu, \qquad (1)$$

where $g_\pi(g_\nu)$ is the g-factor and $L_\pi(L_\nu)$ the angular momentum operator of the proton (neutron) bosons. To test the hypothesis that changes in effective N_π values can account for changes in the underlying shell structure, g_π and g_ν were assumed to be constant over the region of interest. The magnetic moment can then be written as

$$\mu(2^+{}_1) = (8/45\ \pi)^{1/2}\ (g_\nu M_\nu + g_\pi M_\pi), \qquad (2)$$

where M_ν, M_π are the matrix elements of L_ν, L_π. Thus, eq. (2) implies that there should be a linear relationship between μ^{exp}/M_ν and M_π/M_ν. Two different sets of N_π values were used to calculate the matrix elements of M_π and M_ν: one set assumed a major shell for Z = 50-82, the other assumed a Z = 50-64 shell for $N \leq 88$ and a Z = 50-82 shell for $N \geq 90$. The values of M_π and M_ν were found to be essentially independent of all parameters except N_π. The results of these calculations are shown in Fig. 7, and give support to the concept of a proton valence space truncation due to a subshell closure at Z = 64.

These studies are continuing with the use of the new superconducting magnet system at TRISTAN. New measurements in this and other regions of known or suspected subshell closures will be performed to further investigate the use of g-factors to measure effective proton numbers.

Systematics of Intruder States in Cd

The structure of even Cd isotopes was studied, with particular attention to the observation of 0^+ states and their identification as either members of a normal vibration-like configuration or as the head of an intruder band.[10] The results were interpreted in terms of a schematic model calculation involving mixing of normal vibration-like and intruder rotation-like states. The Cd systematics are shown in Fig. 8.

The intruder states are thought to be mainly 2p-4h states resulting from the excitation of a pair of protons across the Z=50 shell gap. Calculations were performed with the IBA-2 in which ^{114}Cd has one proton-boson hole (N_π=1) and eight neutron bosons (N_ν=8). The 2p-4h intruder states were approximated by N_π=3, due to excitation of a pair of protons into the next shell (two boson holes below the gap and one boson above the gap). Both configurations, the normal vibrational (N_π=1) and

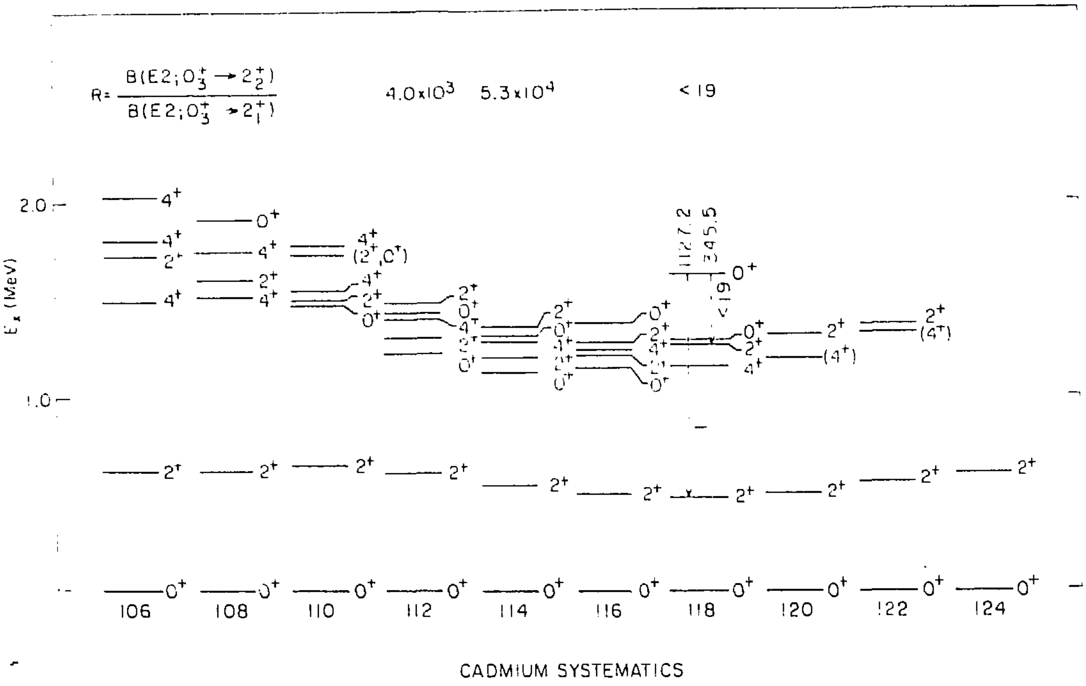

Fig. 8. Systematics of low-lying states in the cadmium nuclei.

K. Wohn and John C. Hill (A=100), A. Wolf and D. D. Warner (g-factors), and A. Aprahamian and R. F. Casten (Cd intruder states) must be recognized. Research has been performed under contract DE-AC02-76CH00016 with the United States Department of Energy.

REFERENCES

1. M. Shmid, R. L. Gill and C. Chung, Nucl. Instr. and Meth. 211, 287 (1983).
2. A. Piotrowski, R. L. Gill and D. C. McDonald, Nucl. Instr. and Meth. (in press).
3. R. L. Gill and A. Piotrowski, Nucl. Instr. and Meth. (to be pub.).
4. A. Wolf, C. Chung, W. B. Walters, G. Peaslee, R. L. Gill, M. Shmid, V. Manzella, E. Meier, M. L. Stelts, H. I. Liou, R. E. Chrien, and D. S. Brenner, Nucl. Instr. and Meth. 206, 397 (1983).
5. R. Kirchner, Nucl. Instr. and Meth. 186, 275 (1981).
6. W. B. Walters, C. Chung, D. S. Brenner, A. Aprahamian, R. L. Gill, R. E. Chrien, M. Shmid, A. Wolf, and L.-J. Yuan, Phys. Lett. 125B, 351 (1983).
7. V. Paar, Nucl. Phys. A331, 16 (1979).
8. F. K. Wohn, John C. Hill, R. F. Petry, H. Bejbakhsh, Z. Berant, an R. L. Gill, Phys. Rev. Lett. 51, 873 (1983).
9. A. Wolf, Z. Berant, D. D. Warner, R. L. Gill, M. Shmid, R. E. Chrien, G. Peaslee, H. Yamamoto, John C. Hill, F. K. Wohn, C. Chung, and W. B. Walters, Phys. Lett. 123B, 165 (1983).
10. A. Aprahamian, D. S. Brenner, R. F. Casten, R. L. Gill, A. Piotrowski, and K. Heyde, Phys. Lett. (in press).

the intruder ($N_\pi=3$) are mixed to calculate the Cd energy spectrum and transition rates.

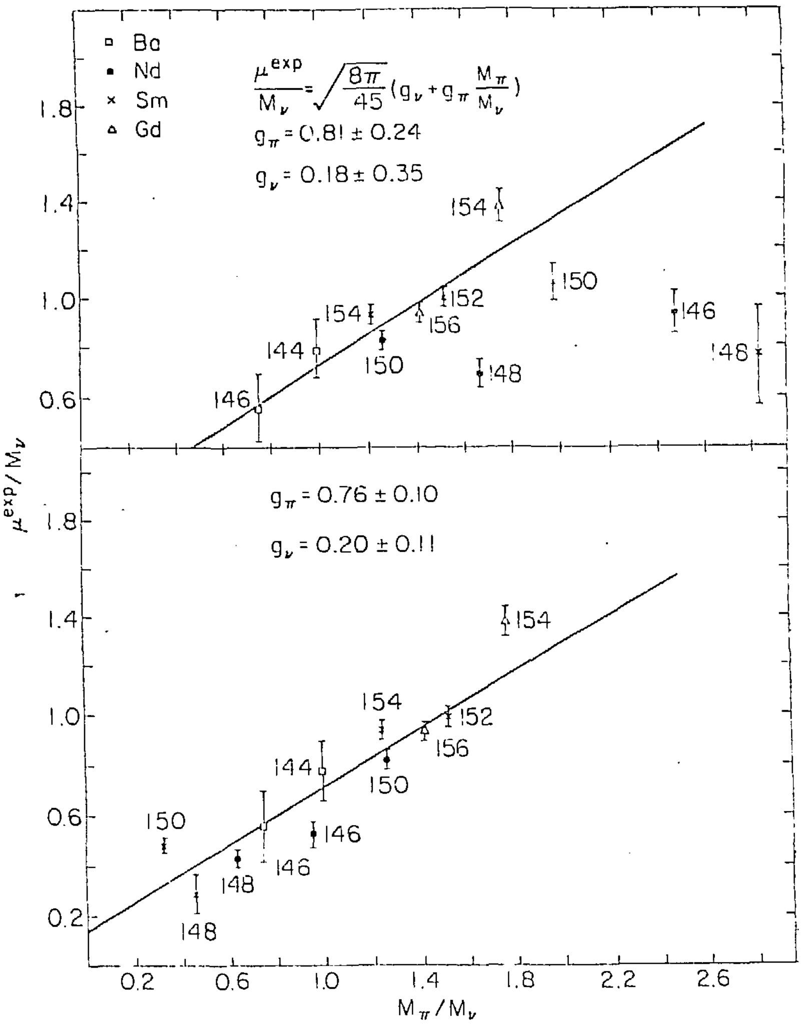

Fig. 7. Values of μ^{exp}/M_ν versus M_π/M_ν for 2^+_1 states in Ba, Nd, Sm and Gd. The upper portion assumes a Z=50-82 shell for all N, whereas the lower portion assumes Z=50-64 for N<88 and Z=50-82 for N>90.

The essential behavior of the intruder states can be understood based on the simple properties of the attractive quadrupole force, which varies as n(n-1). Thus the $Q_\pi \cdot Q_\nu$ term in the IBA-2 Hamiltonian is approximately proportional to $N_\pi N_\nu$. Thus, the normal states with small N_π will be vibration-like, while the intruder states with larger N_π will be more rotation-like and will decrease in energy as N_ν increases toward midshell and rise thereafter. Therefore, the mixing with the normal states will rapidly increase toward the neutron midshell configuration.

As can be seen in Fig. 8, the predicted rise in energy of the 0^+ state associated with the intruder band is indeed observed for the first time. The observation of such a rise strongly supports the basic concept of the coexistence of intruder and vibration-like states. Further experiments in this region are in progress at TRISTAN.

ACKNOWLEDGEMENTS

The author would like to thank the many TRISTAN users who were responsible for much of the work discussed in this paper. In particular, the efforts of A. Piotrowski (ion sources), W. B. Walters (paraboli), F.